Politecnico di Milano

Final degree test:
Introduction to Space Mission Analysis

Academic year 2022-2023

Professor: Andrea Colagrossi

Authors: Group A19		
Person Code	**Surname**	**Name**
10726940	Bachini	Pier Francesco A.
10721571	Belletti	Stefano
10744452	Bertoni	Lorenzo

POLITECNICO
MILANO 1863

SCUOLA DI INGEGNERIA INDUSTRIALE
E DELL'INFORMAZIONE

Submission date: Friday 9th December, 2022

Contents

1 Introduction

The work described in this document is the development of a transfer strategy (e.g. for a satellite) between two given points on different orbits, as part of the Introduction to Space Mission Analysis (final degree test).

The development of the strategies and their animations was made on Matlab® and our functions were implemented to be able to work with almost any given pair of orbits, so that they could be used to test different hypothesis, understanding their weaknesses and limits.

Considering only impulsive maneuvers, the mass ratio (percentage of fuel mass on wet mass) calculation using Tsiolkovsky equation was also implemented for each strategy, thus giving better understanding of plausible implementations in real life situations. The engine impulse used for the calculation is $348s$, which is based on vacuum performance of a Merlin 1D+ engine.

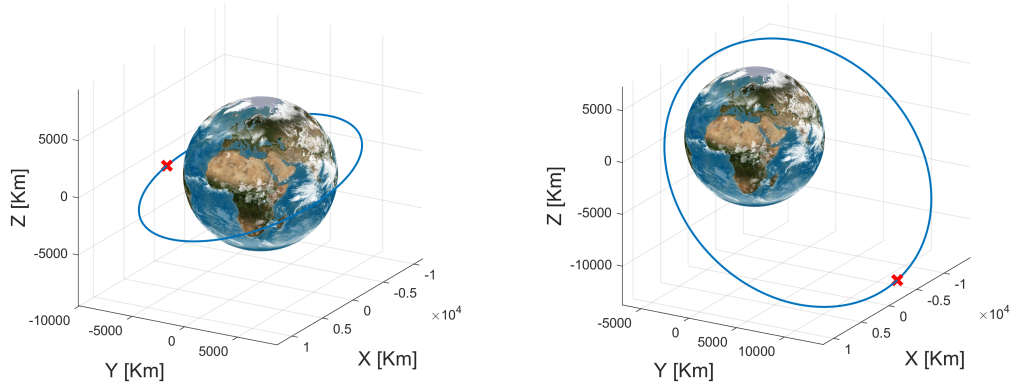

(a) Initial (b) Final

Figure 1: Initial and final orbits

2 Initial orbit characterization

The initial orbit is defined by initial position and velocity vectors within the ECI coordinate system:

$x\ [Km]$	$y\ [Km]$	$z\ [Km]$	$v_x [Km/s]$	$v_y\ [Km/s]$	$v_z\ [Km/s]$
-1788.3462	-9922.9190	-1645.8335	5.6510	-1.1520	-1.8710

To characterize the orbit, we calculated the Keplerian orbital parameters using the function *rv2parorb.m*:

$$\{a,\ e,\ i,\ \Omega,\ \omega,\ \theta\} = \{9658.0703,\ 0.0915,\ 0.3455,\ 0.9218,\ 1.3142,\ 2.3232\}\ [SI\ units]$$

Calculating it's apsidal radii we found that the entire path barely resides in the "MEO" region. Moreover, as the orbit's inclination is less than $\frac{\pi}{2}$, it can be classified as prograde.

The orbit's representation in Figure 1a shows how the orbit's shape tends to a circumference because of it's low eccentricity.

3 Final orbit characterization

To identify the final orbit, we were given the following Keplerian paramenter:

$$\{a, e, i, \Omega, \omega, \theta\} = \{13290.0000,\ 0.3855,\ 0.9526,\ 2.5510,\ 2.2540,\ 3.0360\}\ [SI\ units]$$

The corresponding position and velocity in the ECI coordinate system is calculated using the function *parorb2rv.m*:

$x\ [Km]$	$y\ [Km]$	$z\ [Km]$	$v_x[Km/s]$	$v_y\ [Km/s]$	$v_z\ [Km/s]$
-3360.7862	12979.3399	-12527.3419	-3.2360	0.9160	1.4639

Similar to the initial orbit, this one is still in the "MEO" region. It's also a prograde orbit, as its inclination is less than $\frac{\pi}{2}$.

Interestingly, part of it resides in the inner Van Allen belt. This means that a satellite traveling along this orbit will need to be shielded against the radiation damages it can cause.

From the orbit's representation in Figure 1b, it may be seen that the final point is located slightly before the orbit's apocenter (~ 0.1056 rad less): this had to be taken into account during later analysis, as it meant that every maneuver that reached the final orbit's apocenter would then have to travel almost the entire orbit to reach the ending point.

At the same time, it is visible that the final orbit's shape and plane are very different from the initial ones. Therefore, we could expect costly plane change maneuvers.

4 Transfer trajectories definition and analysis

4.1 Standard strategy

We started our research by implementing the standard strategy the way it was described in the course; it is composed of a series of three maneuvers: plane change, argument of periapsis change and a bitangent maneuver to change the orbit's shape, for a total of four impulses.

As our function *StandardOptimized.m* was made to be able to optimize either for time or cost, we noticed that, while the first two maneuvers were the same, the optimization depended on the type of bitangent used:

Type of bitangent	$\Delta v\ [Km/s]$	$\Delta t\ [s]$	Mass ratio [%]	Optimization
Apocenter - Apocenter	7.6009	33329.2874	89.2164	Δv
Pericenter - Pericenter	7.7407	25639.3816	89.6493	Δt

As expected both strategies suffer from the high cost of the plane change maneuver (around 75% of total cost), thus later analysis will need to focus on reducing it. Moreover, needing to reach the final orbit's apocenter, the Δv optimized strategy has to do almost an entire revolution to reach the ending point (44.15% of total time), which causes the required time to drastically increase.

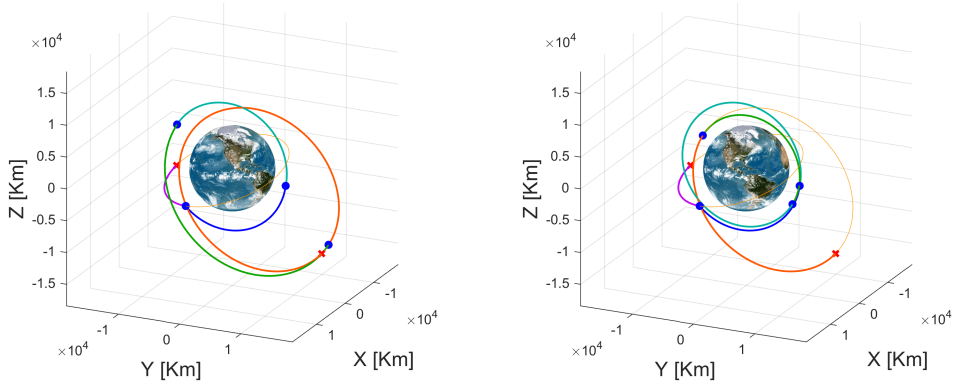

(a) Δv optimized (b) Δt optimized

Figure 2: Standard

4.2 Standard with shape change before plane change

Since the plane change maneuver cost decreases the further it is done from Earth, we decided to try a different approach, still based on the standard strategy: the final orbit is larger than the initial one, so changing the orbit's shape first should reduce the plane change maneuver cost. Thus, the transfer is composed by the following maneuvers: bitangent shape change, plane change and argument of periapsis change.

While this approach can theoretically give us better results, the total cost will be highly affected by the increase of the argument of periapsis change cost. As we did for the standard strategy, we implemented the function *InvertedStandard.m* that can optimize either for cost or time:

Type of bitangent	Δv $[Km/s]$	Δt $[s]$	Mass ratio [%]	Optimization
Pericenter - Apocenter	9.0096	23114.5090	92.8632	Δv
Apocenter - Pericenter	9.0384	22630.7839	92.9233	Δt

From the results gathered we saw that this maneuver was actually less effective than the Standard strategy, as the argument of periapsis change cost increase outweighs the benefit of the plane change cost reduction.

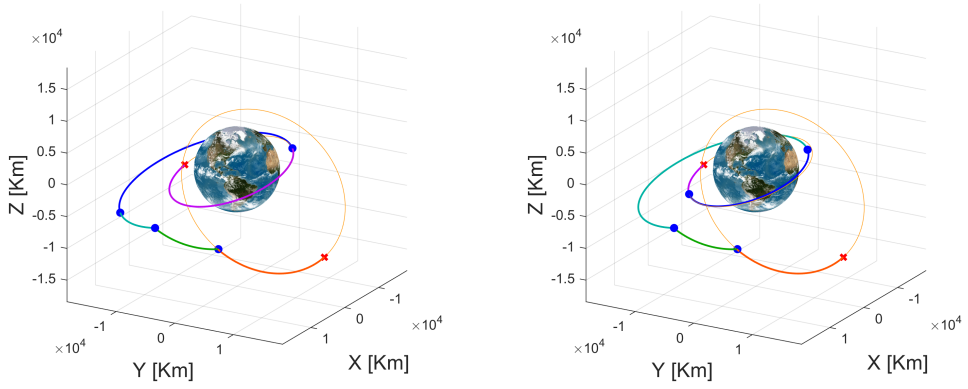

(a) Δv optimized (b) Δt optimized

Figure 3: Inverted Standard

4.3 Direct

To work around this problem, we decided to implement a transfer that would move the satellite from the starting to the ending points using an orbit that connects the two, thus needing only two impulses. Thanks to our function *twoPointsOrbit.m*, we were able to generate an orbit that would connect two arbitrarily given points (with some constraints); feeding it with the initial and final points, we obtained the direct transfer between them. As the function *DirectOptimized.m* was made to optimize either for cost or time, we tested both with same results:

Δv $[Km/s]$	Δt $[s]$	Mass ratio [%]
14.3652	6700.1589	98.5141

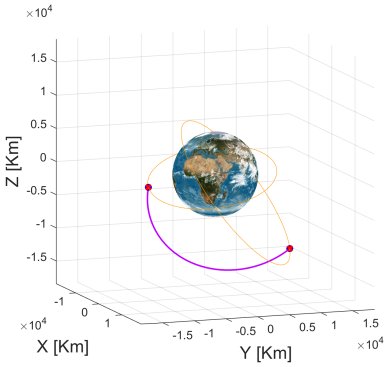

Figure 4: Direct

The cost of the maneuver is really high: this comes from the fact that the transfer orbit generated has a high inclination difference with both the initial and the final orbit, thus making the maneuver almost impracticable.

4.4 Direct transfer with cost optimization

As the direct strategy proved to be really time efficient, we decided to keep working on a two impulse strategy, trying to find the transfer orbit that would minimize the cost, while keeping the time as low as possible. To help in the process, we created the functions *nearFinder.m* and *low_dv_finder.m* that iteratively found the points from where the transfer orbit would have the lowest cost (with some constraints, mostly based on time).
The resulting points on their respective orbits were: $\{\theta_i,\ \theta_f\} = \{3.4732,\ 1.3823\}\ [rad]$.

Using these values, the results are as follows:

$\Delta v\ [Km/s]$	$\Delta t\ [s]$	Mass ratio [%]
6.6324	7971.6116	85.6779

As expected, the obtained maneuver is still efficient in terms of total time, while reducing the cost to the minimum found so far.

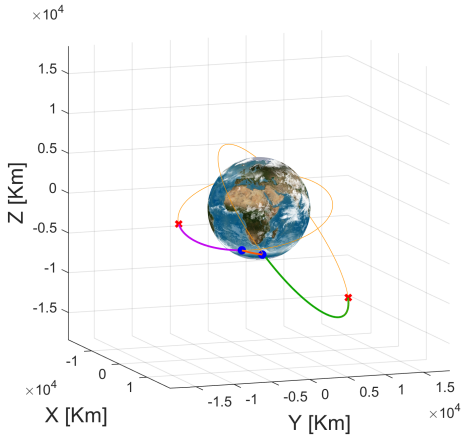

Figure 5: Direct Δv_{min}

4.5 Bielliptic

With the direct maneuvers we ended up optimizing time first and then cost. This time, we decided to try constructing a strategy whose sole focus was to reduce cost. To do this we used a bielliptic transfer: a three impulses strategy that starts by enlarging the initial orbit, then uses a direct transfer to reach the final point. To decide the initial and final points, as well as the apogee radius, we performed various tests, all condensed in the script *BiellipticTests.m*. The final chosen configuration was: starting at the initial orbit's perigee, ending at the final point, using an apogee radius of 57'000 Km (for the transfer orbit). The chosen apogee radius was the one that minimized the total cost, as can be seen in Figure 6a.

The total results are:

$\Delta v\ [Km/s]$	$\Delta t\ [s]$	Mass ratio [%]
7.1918	66417.6263	87.8432

The findings weren't what we hoped for. This was due to a couple of unforeseen problems: as the initial orbit's eccentricity is so low, changing it to a higher value (e_{tras} *is* 8 *times* e_i) was more costly than expected; at the same time, the last maneuver's cost is lower than any change plane analyzed so far, but still high enough to leave this strategy less effective than the Direct transfer with cost optimization.

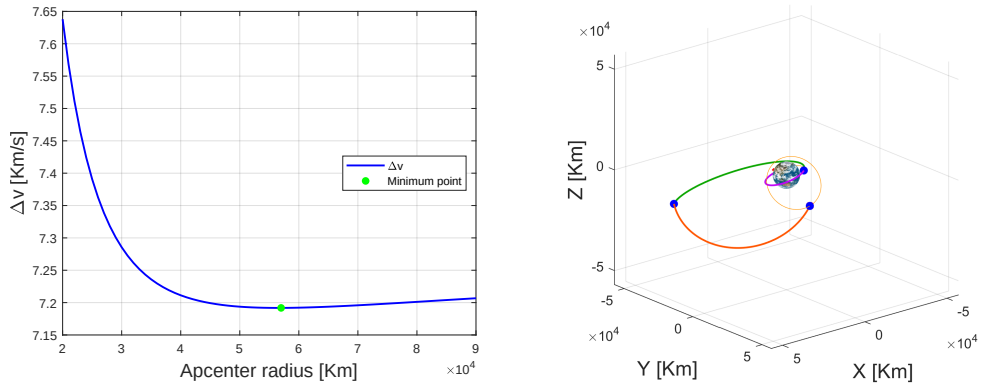

(a) Δv over radius (b) Bielliptic

Figure 6: Bielliptic

4.6 Intersection

This last strategy was born from an observation we made during the development of the Bielliptic strategy: the initial and final orbits are close enough (the nearest points are distant *around* 130 Km) to allow us to slightly enlarge the first one so that it intersects the other. This led to the development of a new two impulses strategy composed of: a maneuver at the starting point to enlarge the initial orbit and a second impulse at the intersection point with the final orbit.
Using the script and the function *Intersection.m* we found the points on the two orbits, while the *twoPointsOrbit.m* function generated the transfer orbit, obtaining this results:

Δv $[Km/s]$	Δt $[s]$	Mass ratio [%]
7.0185	7816.0531	87.2099

This transfer proved to be surprisingly efficient, both in terms of cost and time, even if the plane change maneuver was really expensive, because of the different inclination of the two orbits, as noticed in the Final orbit characterization

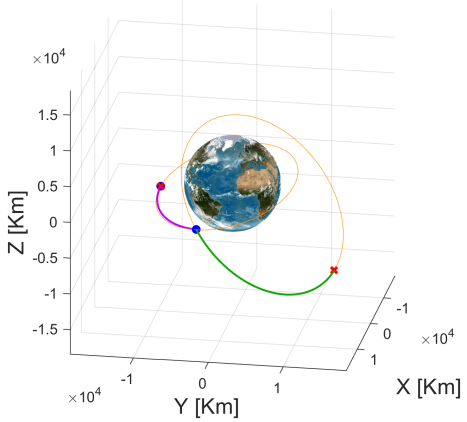

Figure 7: Intersection

5 Conclusions

As we can see from Figure 8, the least expensive maneuver is the Direct with cost optimization strategy with a total Δv of 6.6324 km/s, whereas the least time consuming one is the Direct strategy with a total time of 6700.2 seconds (or 1.86 hours).

However, looking at the total Δv of the Direct maneuver, we can classify this strategy as not viable due to its high cost (14.3652 km/s). Studying it was still fundamental, as from its optimization was born the Direct with cost optimization strategy

As almost all space missions need to be as cost efficient as possible, the need to reduce the Δv has to be a priority. In fact, as the weight of the payload increases, the ratio of propellant to total mass grows closer to 1, thus creating economic and structural complexity problems. For example, the difference between the Direct and the Direct Δv_{min} is: $(m_{fuel}/m_{wet})_{Direct} = 0.9851$ (66.3003 kg of propellant per 1Kg of dry mass), whereas $(m_{fuel}/m_{wet})_{\Delta v_{min}} = 0.8568$ (5.9822 kg of propellant per 1Kg of dry mass).

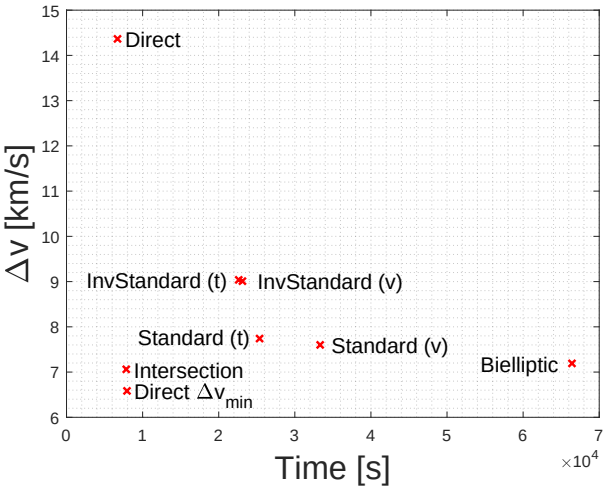

Figure 8: Comparison

For this reason, in the end, the chosen maneuver was the one that better balances low cost with optimal transfer time: the Direct with cost optimization strategy.

This strategy is the most viable we were able to find according to our capabilities and understandings. This implementation on MatLab® also gave us a better understanding on computational power and resources needed to find a solution to our problems. All the code written for this report is commented and documented for a better comprehension.

6 Appendix

Standard Transfer (Bitangent A-A) - Δv optimized							
t [s]	a [km]	e [-]	i [rad]	Ω [rad]	ω [rad]	θ [rad]	Δv [km/s]
0	9658.0703	0.0915	0.3455	0.9218	1.3142	2.3232	-
2411.2469	9658.0703	0.0915	0.3455	0.9218	1.3142	3.6863	5.7700
	9658.0703	0.0915	0.9526	2.5510	6.1483	3.6863	
5693.1925	9658.0703	0.0915	0.9526	2.5510	6.1483	5.9068	0.4341
	9658.0703	0.0915	0.9526	2.5510	5.3956	0.3764	
9945.3806	9658.0703	0.0915	0.9526	2.5510	5.3956	π	1.0738
	14477.7274	0.2718	0.9526	2.5510	2.2540	0	
18613.6384	14477.7274	0.2718	0.9526	2.5510	2.2540	π	0.3230
	13290.0000	0.3855	0.9526	2.5510	2.2540	π	
33329.2874	13290.0000	0.3855	0.9526	2.5510	2.2540	3.0360	-

Standard Transfer (Bitangent P-P) - Δt optimized							
t [s]	a [km]	e [-]	i [rad]	Ω [rad]	ω [rad]	θ [rad]	Δv [km/s]
0	9658.0703	0.0915	0.3455	0.9218	1.3142	2.3232	-
2411.2469	9658.0703	0.0915	0.3455	0.9218	1.3142	3.6863	5.7700
	9658.0703	0.0915	0.9526	2.5510	6.1483	3.6863	
5693.1925	9658.0703	0.0915	0.9526	2.5510	6.1483	5.9068	0.4341
	9658.0703	0.0915	0.9526	2.5510	5.3956	0.3764	
14668.3678	9658.0703	0.0915	0.9526	2.5510	5.3956	0	0.4237
	8470.3429	0.0358	0.9526	2.5510	2.2540	π	
18547.4834	8470.3429	0.0358	0.9526	2.5510	2.2540	0	1.1130
	13290.0000	0.3855	0.9526	2.5510	2.2540	0	
25639.3816	13290.0000	0.3855	0.9526	2.5510	2.2540	3.0360	-

Inverted standard (Bitangent P-A) - Δv optimized							
t [s]	a [km]	e [-]	i [rad]	Ω [rad]	ω [rad]	θ [rad]	Δv [km/s]
0	9658.0703	0.0915	0.3455	0.9218	1.3142	2.3232	-
6163.9915	9658.0703	0.0915	0.3455	0.9218	1.3142	0	0.8027
	13593.6379	0.3546	0.3455	0.9218	1.3142	0	
14050.5000	13593.6379	0.3546	0.3455	0.9218	1.3142	π	0.0907
	13290.0000	0.3855	0.3455	0.9218	1.3142	π	
16644.9338	13290.0000	0.3855	0.3455	0.9218	1.3142	3.6863	3.8604
	13290.0000	0.3855	0.9526	2.5510	6.1483	3.6863	
18848.4308	13290.0000	0.3855	0.9526	2.5510	6.1483	4.3360	4.2558
	13290.0000	0.3855	0.9526	2.5510	2.2540	1.9472	
23114.5090	13290.0000	0.3855	0.9526	2.5510	2.2540	3.0360	-

Inverted standard (Bitangent A-P) - Δt optimized							
t [s]	a [km]	e [-]	i [rad]	Ω [rad]	ω [rad]	θ [rad]	Δv [km/s]
0	9658.0703	0.0915	0.3455	0.9218	1.3142	2.3232	-
1441.0043	9658.0703	0.0915	0.3455	0.9218	1.3142	π	0.1154
	9354.4324	0.1270	0.3455	0.9218	1.3142	π	
5943.0240	9354.4324	0.1270	0.3455	0.9218	1.3142	0	0.8068
	13290.0000	0.3855	0.3455	0.9218	1.3142	0	
16161.2087	13290.0000	0.3855	0.3455	0.9218	1.3142	3.6863	3.8604
	13290.0000	0.3855	0.9526	2.5510	6.1483	3.6863	
18364.7057	13290.0000	0.3855	0.9526	2.5510	6.1483	4.3360	4.2558
	13290.0000	0.3855	0.9526	2.5510	2.2540	1.9472	
22630.7839	13290.0000	0.3855	0.9526	2.5510	2.2540	3.0360	-

Direct (Starting - Ending points)							
t [s]	a [km]	e [-]	i [rad]	Ω [rad]	ω [rad]	θ [rad]	Δv [km/s]
0	9658.0703	0.0915	0.3455	0.9218	1.3142	2.3232	-
0	9658.0703	0.0915	0.3455	0.9218	1.3142	2.3232	9.4736
	13692.9154	0.3400	1.9389	1.4555	2.3207	0.9944	
6700.1589	13692.9154	0.3400	1.9389	1.4555	2.3207	π	4.8916
	13290.0000	0.3855	0.9526	2.5510	2.2540	3.0360	
6700.1589	13290.0000	0.3855	0.9526	2.5510	2.2540	3.0360	-

Direct optimized for Δv_{min}							
t [s]	a [km]	e [-]	i [rad]	Ω [rad]	ω [rad]	θ [rad]	Δv [km/s]
0	9658.0703	0.0915	0.3455	0.9218	1.3142	2.3232	-
2035.3146	9658.0703	0.0915	0.3455	0.9218	1.3142	3.4732	1.6688
	9142.7952	0.1542	0.4218	1.6458	1.2376	2.8739	
2532.9570	9142.7952	0.1542	0.4218	1.6458	1.2376	π	4.9636
	13290.0000	0.3855	0.9526	2.5510	2.2540	1.3823	
7971.6116	13290.0000	0.3855	0.9526	2.5510	2.2540	3.0360	-

Bielliptic							
t [s]	a [km]	e [-]	i [rad]	Ω [rad]	ω [rad]	θ [rad]	Δv [km/s]
0	9658.0703	0.0915	0.3455	0.9218	1.3142	2.3232	-
6163.9915	9658.0703	0.0915	0.3455	0.9218	1.3142	0	1.8316
	32886.9904	0.7332	0.3455	0.9218	1.3142	0	
35840.8157	32886.9904	0.7332	0.3455	0.9218	1.3142	π	1.6927
	35658.8796	0.5985	1.2737	2.1143	0.3497	π	
66417.6263	35658.8796	0.5985	1.2737	2.1143	0.3497	5.1383	3.6675
	13290.0000	0.3855	0.9526	2.5510	2.2540	3.0360	
66417.6263	13290.0000	0.3855	0.9526	2.5510	2.2540	3.0360	-

Intersection							
t [s]	a [km]	e [-]	i [rad]	Ω [rad]	ω [rad]	θ [rad]	Δv [km/s]
0	9658.0703	0.0915	0.3455	0.9218	1.3142	2.3232	-
0	9658.0703	0.0915	0.3455	0.9218	1.3142	2.3232	0.4434
	10205.1187	0.0055	0.3483	0.9262	1.8566	1.7766	
2246.4291	10205.1187	0.0055	0.3483	0.9262	1.8566	π	6.5751
	13290.0000	0.3855	0.9526	2.5510	2.2540	1.3011	
7816.0531	13290.0000	0.3855	0.9526	2.5510	2.2540	3.0360	-

7 Academic Honesty

Earth's flat image used for 3d representations and animations was downloaded from Nasa website as there's no restrictions under "Still Images, Audio Recordings, Video, and Related Computer Files for Non-Commercial Use" for our use. We do not own this image: NASA/Goddard Space Flight Center Scientific Visualization Studio The Blue Marble Next Generation data is courtesy of Reto Stockli (NASA/GSFC) and NASA's Earth Observatory.

Moreover we did not use any external package other than stock MatLab® install.